Drag Reduction by Leidenfrost Vapor Layers

Ivan U. Vakarelski,[1,2,*] Jeremy O. Marston,[1] Derek Y. C. Chan,[3,4] and Sigurdur T. Thoroddsen[1,5]

[1]*Division of Physical Sciences and Engineering, King Abdullah University of Science and Technology,
Thuwal 23955-6900, Saudi Arabia*
[2]*Institute of Chemical and Engineering Sciences, 1 Pesek Road, 627833 Singapore*
[3]*Department of Mathematics and Statistics, University of Melbourne, Parkville VIC 3010, Australia*
[4]*Faculty of Life and Social Sciences, Swinburne University of Technology, Hawthorn VIC 3122, Australia*
[5]*Clean Combustion Research Center, King Abdullah University of Science and Technology, Thuwal 23955-6900, Saudi Arabia*

We demonstrate and quantify a highly effective drag reduction technique that exploits the Leidenfrost effect to create a continuous and robust lubricating vapor layer on the surface of a heated solid sphere moving in a liquid. Using high-speed video, we show that such vapor layers can reduce the hydrodynamic drag by over 85%. These results appear to approach the ultimate limit of drag reduction possible by different methods based on gas-layer lubrication and can stimulate the development of related energy saving technologies.

Novel methods to reduce hydrodynamic drag are crucial to efficient energy usage with applications from naval architectural design to the operation of microfluidic devices. One innovative approach to achieve drag reduction on a solid body moving in liquid is to introduce a lubricating gas layer between the body surface and the surrounding liquid by deploying superhydrophobic surfaces [1–7], microbubble injection [8,9], or supercavitation [9]. Because of the different morphology of the gas layer and the wide range of shapes, sizes, and operating velocities of the moving bodies, the drag reduction that can be achieved vary from significant [8–10] to moderate to even being counterproductive [3]. Here we demonstrate that the Leidenfrost effect can sustain a continuous and robust lubricating layer on the surface of fast moving solid sphere in fluids. The resulting drag reduction approaches the ultimate limit that can be induced by gas layers.

When a small drop of liquid is placed on a very hot surface whose temperature is significantly above the boiling point of the liquid, a vapor layer can be sustained between the drop and the surface and insulates the drops against further evaporation. The drop is thus levitated above the hot surface and becomes extremely mobile [11] because of the efficient lubricating effect of the vapor layer. This phenomenon, known as the Leidenfrost effect [12], was observed and understood over 250 years ago. More recently, it has been exploited in fundamental studies of noncontact collisions between a drop and a surface [13,14], nanopatterning [15] and more generally is responsible for the undesirable side effects associated with the loss of cooling in automobile radiators as well as nuclear reactors. The temperature (T_L) at which the Leidenfrost effect occurs has a complex dependence on material properties and has been shown to be substantially lower on superhydrophobic surfaces [16].

If we now invert the geometry by considering a body that has been heated above T_L and then immersed in a fluid, we can investigate the drag reduction effect of the associated Leidenfrost vapor layer that forms on the surface of the body. Owing to the symmetry and practical relevance, the hydrodynamic drag on a moving sphere has been studied extensively and the effect is commonly characterized in terms of the drag coefficient, $C_D = 2F_D/(\pi R^2 \rho U^2)$, that has a universal dependence on the Reynolds number, $\mathrm{Re} = 2\rho R U/\mu$. Here, F_D is the drag force on the sphere, U is the sphere velocity, ρ is the fluid density, R is the sphere radius and μ is the fluid shear viscosity. There are two contributions to hydrodynamic drag: skin friction due to the fluid viscosity and pressure-induced drag referred as wake or form drag. The drag coefficient for a solid sphere with the "stick" or no-slip boundary condition at low velocities that corresponds to a low Reynolds number regime, $\mathrm{Re} < 0.5$, has the form $C_D = 24/\mathrm{Re}$, which follows from the Stokes formula: $F_D = 6\pi\mu RU$. At high velocities or large Re, there is no analytical result, but experimental observations indicate that C_D decreases and deviates from the Stokes result until the so-called subcritical range $5 \times 10^3 \leq \mathrm{Re} \leq 3 \times 10^5$, where flow around a solid sphere is characterized by flow separation occurring at about the equator of the sphere. Within this subcritical range of Re, the wake drag contribution is dominant and the drag coefficient is approximately constant: $C_D \approx 0.44$. At a critical value, $\mathrm{Re} \approx 3.5 \times 10^5$, the boundary layer becomes turbulent and results in a delayed separation of the wake and is accompanied by a dramatic reduction in the drag coefficient to $C_D \approx 0.1$ [17]. The objective of this Letter is to investigate the effects of a Leidenfrost vapor layer on the drag coefficient of a solid sphere falling freely under gravity in the subcritical range of the Reynolds number $5 \times 10^3 \leq \mathrm{Re} \leq 3 \times 10^5$.

If the solid-liquid interface of the sphere is replaced by an ideal nondeformable spherical gas-liquid interface where it is assumed to have zero tangential stress, the drag coefficient has the form $C_D = 16/Re$ at low Reynolds number that follows from the Hardamard-Rubczynski formula: $F_D = 4\pi\mu RU$, for $Re \rightarrow 0$; and has the theoretical limiting form $C_D = 48/Re$, for $Re \rightarrow \infty$ as obtained by Levich [18]. However, deformation of the gas-liquid interface has a significant effect on the drag coefficient at large Re [19] so the Levich result is not observed in practice [20]. The present experimental technique offers an alternative methodology to probe the drag on a nondeformable "bubble" at larger Re.

We produce an inverted Leidenfrost effect by immersing a metallic sphere, heated to an initial temperature T_S, in a liquid with a low vaporization heat capacity. The perfluorinated liquid we used, FC-72 (3M™ Fluorinert™ Electronic Liquid, mostly composed of perfluorohexane, C_6F_{14}) has a boiling point of 56 °C and a vaporization heat capacity that is approximately 30 times lower than that of water. Figure 1 shows snapshots of the states of fluid motion associated with the cooling of a stationary steel sphere (initial temperature $T_S = 250$ °C) suspended magnetically in the FC-72 liquid. When first immersed in the liquid, a continuous thin vapor layer forms around the sphere, evident by the rippling waves moving along the sphere surface accompanied by periodic release of bubbles from the upper pole of the sphere [Fig. 1(a)]. The vapor layer thickness estimated by high magnification imaging at the sphere surface was found to be in the range of 100 to 200 μm (see supplemental materials Fig. 3S [21]). After the sphere temperature cools below the Leidenfrost temperature, T_L, of about 130 °C, in about 25 sec. in this case, the continuous vapor layer surrounding the sphere can no longer be maintained and the fluid comes into direct contact with the hot sphere surface. This point is marked by a very dramatic and explosive release of bubbles [Fig. 1(b)]. The entire sphere cooling process can be seen in the supplemental video 1 [21].

In our moving sphere experiments, a sphere is heated in a temperature-controlled furnace and then released to fall freely under gravity in a cylindrical tank with height of 2 m and diameter of 80 mm filled with the perfluorinated liquid. The subsequent motion is captured with a high-speed camera to determine the terminal velocity, U. The drag coefficient of the sphere can then be calculated from the balance between gravity, buoyancy and drag forces as: $C_D = (8g[\rho_s - \rho]R)/(3\rho U^2)$, where g is the gravitational acceleration, ρ_s is the sphere density and ρ is the liquid density (See supplemental material for experimental details and notes on the drag coefficient derivation accounting for the cylinder wall effects [21]).

In Fig. 2 we show the dependence of the terminal velocity of a 20 mm diameter steel sphere with sphere temperatures in the range: 25 °C $< T_S <$ 280 °C. The data clearly demonstrate the dramatic effect due to the onset of the Leidenfrost regime. An initial increase in sphere temperature from 25 °C to 110 °C results in a moderate increase in the terminal velocity of about 20% in the range 1.3 m/s to 1.6 m/s. Such variations could be due to a confluence of the heat-induced viscosity change of the surrounding fluid and the partial coverage of the sphere with bubbles when the sphere temperature is above the boiling point of the fluid. However, when the sphere temperature exceeds the Leidenfrost temperature, $T_L = 130$ °C, we observe an increase in the terminal velocity by a factor of 2.6 to a nearly constant value of about
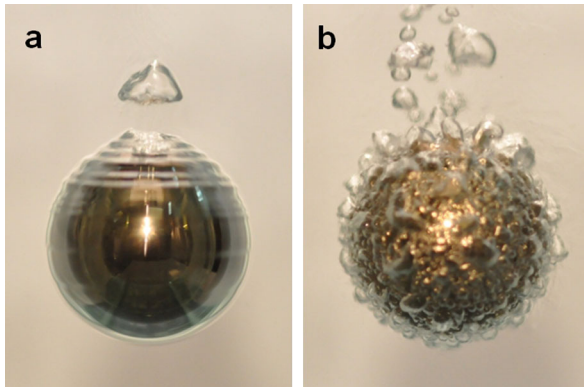

FIG. 1 (color online). (a) Digital camera snapshot of a heated 15 mm steel sphere held stationary in fluorinated liquid with sphere temperature T_S above the Leidenfrost temperature T_L. A thin vapor layer streaming around the sphere can be observed by the ripples moving along the sphere surface. (b) Snapshot at the instant when the sphere has cooled to the Leidenfrost temperature that is marked by an explosive release of bubbles. (See supplemental video 1 [21]).
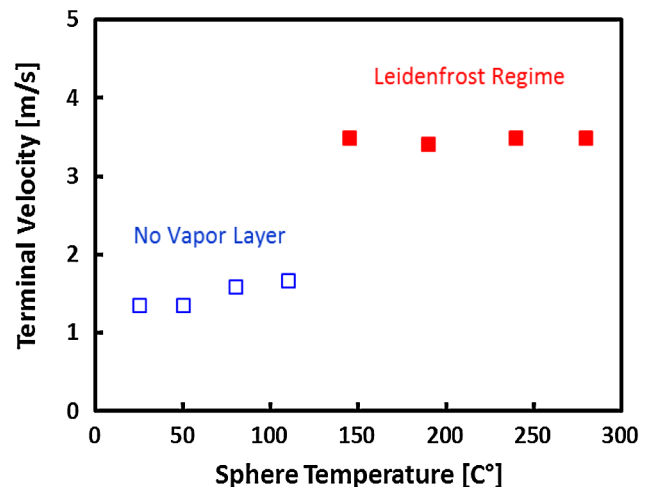

FIG. 2 (color online). Variation of the terminal velocity with the sphere temperature measured for a 20 mm steel sphere falling through the liquid (FC-72). Open square data points (blue) are for temperature below the Leidenfrost temperature ($T_L = 130$ °C) and solid square (red) for temperature above T_L (see supplemental video 2 [21]).

3.5 m/s over the temperature range examined (140 °C < T_S < 280 °C). The dramatic speed difference is illustrated in the supplemental material video 2 [21]. Within the Leidenfrost regime, the terminal velocity is not a sensitive function of the temperature. Over the duration of the experiment, we estimate that the spheres cooled by no more than 7 °C thus ensuring that the spheres remain in the Leidenfrost regime at all times [21].

To further explore the effect of the Leidenfrost vapor layer over a broader range of Reynolds numbers, we performed experiments using spheres with diameters from 5 to 30 mm and made from materials of different mass densities: tungsten carbide (ρ_s = 14 g/cm³), agate (ρ_s = 2.8 g/cm³), and steel (ρ_s = 7.8 g/cm³). In addition, to demonstrate the universality of the vapor layer effect, some "reverse" experiments were carried out with a pulley and counterweight system to pull the spheres upward through the liquid that enabled us to measure the drag coefficient on ascending spheres instead of spheres in free-fall under gravity (see supplemental material for experimental details and video 3 [21]). The results of these experiments are summarized in Fig. 3(a). The drag coefficients for experiments with spheres at room temperature are in accord with values found in the literature [17]

for subcritical Reynolds numbers (Re < 10⁵) with 0.43 < C_D < 0.50. In the Leidenfrost regime, the variation of C_D with Re appears to follow a universal curve that subsumes the effect of the sphere size and density. Experiments with ascending spheres show a similar, albeit slightly weaker dependence on Re indicating that gravity-driven effects, that is, the natural convection of the vapor layer, does not have a significant contribution to the drag reduction mechanism.

The effectiveness of a Leidenfrost vapor layer on reducing the drag coefficient can thus be divided into 3 regimes: (a) low Reynolds numbers (Re up to ~2 × 10⁴), there is negligible effect on C_D, (b) intermediate Reynolds numbers (2 × 10⁴ ≤ Re ≤ 1 × 10⁵), there is a continuous reduction in C_D from 0.45 to 0.1 with increasing Re and (c) higher Reynolds number (Re > 1 × 10⁵), the drag coefficient attains a low limiting value C_D ≈ 0.07. Up to the highest Re investigated here, the drag coefficient can be reduced by about 85% compared with the cold sphere case.

Finally, we adduce evidence for the physical mechanism that underpins drag reduction due to presence of the Leidenfrost vapor layer. For the range of Reynolds numbers investigated herein, the pressure-induced form drag account for around 97% of the total drag on a solid sphere whereas the skin friction is responsible for the remaining 3% [17]. Therefore the presence of the Leidenfrost vapor layer must have modified the form drag on the sphere and effects of the skin friction remains small. Indeed this can be demonstrated by comparing frames from high-speed movies of the spheres falling with terminal velocity at temperatures just below [Fig. 4(a)] or above the Leidenfrost temperature in the case of fully developed drag reduction effect [Fig. 4(c)], and for the intermediate case of a sphere at above the Leidenfrost temperature traveling at a lower
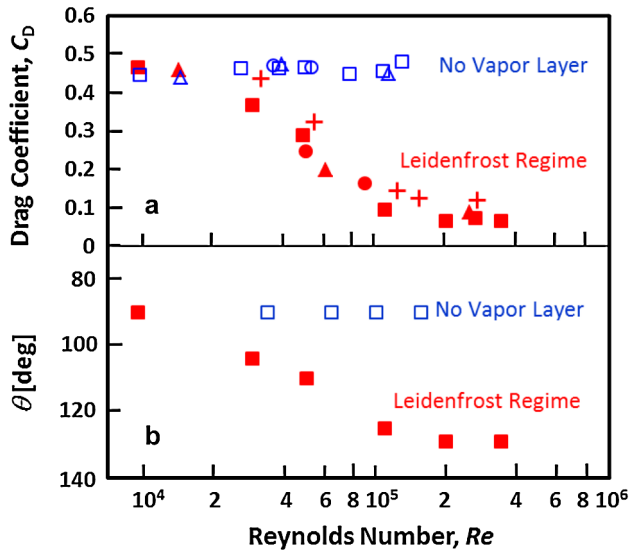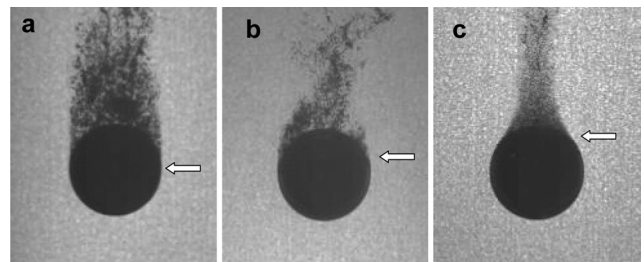

FIG. 3 (color online). (a) Dependence of the drag coefficient on the Reynolds number for different sphere diameters and densities [21]. Open (blue) data points are taken at room temperature (25 °C) for steel (square), tungsten carbide (triangles) and agate (circles) spheres of varying sizes. Solid (red) data points (same symbols) are for the same spheres heated to 200 °C. Data for the heated, ascending steel sphere (red crosses) are also included for comparison. (b) Dependence of the observed separation angle, θ of the boundary layer on the Reynolds number (the bottom pole of the falling sphere is θ = 0). Open squares (blue) are for steel sphere at temperature just below the T_L (T_S = 110 °C) and the solid squares (red) for the same spheres heated to 200 °C (see also Fig. 4).

FIG. 4. Snapshots of 20 mm steel sphere falling at different temperatures and velocities. (a) Sphere temperature, T_S = 110 °C slightly below the Leidenfrost temperature (T_L = 130 °C) with no continuous vapor layer on the sphere surface and terminal velocity U = 1.7 m/s (Re = 7.6 × 10⁴). (b) Sphere temperature, T_S = 200 °C, above Leidenfrost temperature with a continuous vapor layer on the sphere surface but prior to reaching terminal velocity at U = 0.9 m/s (Re = 5.0 × 10⁴). (c) Sphere temperature, T_S = 200 °C, above Leidenfrost temperature and having reached terminal velocity of U = 3.6 m/s (Re = 2.0 × 10⁵). Arrows indicate the approximate position at which flow separation occurs (See supplemental video 4 [21]).

speed prior to reaching the terminal velocity [Fig. 4(b)]. In these silhouette images, the bubbles released act as tracer particles in the wake and help to identify the locations of flow separation on the sphere surface (marked by the arrows). When the sphere temperature is below the Leidenfrost temperature [Fig. 4(a)] we observe a typical subcritical wake with flow separation occurring close to the equator of the sphere ($\theta \approx 90°$), shedding vortex rings in the wake [22]. In contrast, for $T_S > T_L$ [Fig. 4(c)] with a high terminal velocity or Reynolds number, the separation point moves to the rear hemisphere ($\theta \approx 130°$) and the wake appears more streamlined (see supplemental video 4 [21]). The observed variation of the angular position of the boundary layer separation point with Reynolds number mirrors the sixfold decrease in drag coefficient, from $C_D = 0.44$ to $C_D = 0.07$ [Figs. 3(a) and 3(b)]. This drag reduction is similar in magnitude to that observed for the transition from subcritical to supercritical Reynolds numbers [17]. Hence, we can conclude that the Leidenfrost drag reduction mechanism can be attributed to the delayed flow separation and the associated change in the pressure distribution around the sphere.

The observed movement of the separation point appears to be consistent with the high Re calculation of the angular dependence of the boundary layer thickness, $(2\chi(\theta)/\mathrm{Re})^{1/2}R$, for an ''ideal spherical bubble'' that satisfies the zero tangential shear stress on the surface, where $\chi(\theta) = (4 - 6\cos\theta + 2\cos^3\theta)/(9\sin^4\theta)$ [23]. The boundary layer thickness shows a rapid increase in thickness at $\theta \sim 130°$ and coincides with the point of boundary layer separation observed in Fig. 4(c). Thus the vapor layer changes the boundary condition from no-slip to shear-free which reduces the momentum defect in the boundary layer and moves the separation point against the adverse pressure gradient towards the downstream side of the sphere [22].

While previous studies have shown that the introduction of an attached gas layer, for example, through the use of a superhydrophobic surface, can dramatically reduce the skin friction contribution to the overall hydrodynamic drag, for the case of a bluff body this is only effective at relatively low Reynolds numbers where skin friction makes the dominant contribution to the drag force. In this study, we used the Leidenfrost effect to show that a uniform and continuous vapor layer significantly alters the dominant form drag on the sphere over a range of Re, where the skin friction plays a small role. This Leidenfrost-induced drag reduction produced using a two-century old idea, has the potential to stimulate further development of novel drag reduction techniques involving gas layers.

----

*ivanuriev.vakarelski@kaust.edu.sa

[1] C. Cottin-Bizonne, J.-L. Barrat, L. Bocquet, and E. Charlaix, Nature Mater. **2,** 237 (2003).
[2] E. Lauga and H. A. Stone, J. Fluid Mech. **489,** 55 (2003).
[3] A. Steinberger, C. Cottin-Bizonne, P. Kleimann, and E. Charlaix, Nature Mater. **6,** 665 (2007).
[4] B. M. Borkent et al., Phys. Rev. Lett. **98,** 204502 (2007).
[5] G. McHale, M. I. Newton, and N. J. Shirtcliffe, Soft Matter **6,** 714 (2010).
[6] J. P. Rothstein, Annu. Rev. Fluid Mech. **42,** 89 (2010).
[7] C. Lee and C.-J. Kim, Phys. Rev. Lett. **106,** 014502 (2011).
[8] B. R. Elbing et al., J. Fluid Mech. **612,** 201 (2008).
[9] S. L. Ceccio, Annu. Rev. Fluid Mech. **42,** 183 (2010).
[10] M. E. McCormick and R. Battacharyya, Nav. Eng. J. **85,** 11 (1973).
[11] H. Linke et al., Phys. Rev. Lett. **96,** 154502 (2006).
[12] J. G. Leidenfrost, De Aquae Communis Nonnullis Qualitatibus Tractatus (1756); J. G. Leidenfrost, Intl. J. Heat and Mass Transfer **9,** 1153 (1966).
[13] D. Richard, C. Clanet, and D. Quere, Nature (London) **417,** 811 (2002).
[14] A. L. Biance et al., J. Fluid Mech. **554,** 47 (2006).
[15] M. Elbahri et al., Adv. Mater. **19,** 1262 (2007).
[16] G. Liu and V. S. J. Craig, Faraday Discuss. **146,** 141 (2010).
[17] E. Achenbach, J. Fluid Mech. **54,** 565 (1972).
[18] V. G. Levich, Sov. Phys. JETP **19,** 18 (1949).
[19] D. W. Moore, J. Fluid Mech. **23,** 749 (1965).
[20] P. C. Duineveld, J. Fluid Mech. **292,** 325 (1995).
[21] See supplemental material at http://link.aps.org/supplemental/10.1103/PhysRevLett.106.214501 for experimental details, notes on the drag coefficient determination, video clips legends, and video clips (Video 1, Video 2, Video 3, and Video 4).
[22] H. Schlichting, *Boundary Layer Theory* (McGraw-Hill Book Company, New York, 1979).
[23] D. W. Moore, J. Fluid Mech. **16,** 161 (1963).